Integration of coal gasification and packed bed CLC for high efficiency and near-zero emission power generation

V. Spallina [a], M.C. Romano [b,*], P. Chiesa [b], F. Gallucci [a], M. van Sint Annaland [a], G. Lozza [b]

[a] *Chemical Process Intensification, Chemical Engineering and Chemistry, Eindhoven University of Technology, Eindhoven, The Netherlands*
[b] *Group of Energy Conversion Systems, Department of Energy, Politecnico of Milano, Milano, Italy*

Received 7 February 2014
Received in revised form 11 April 2014
Accepted 26 April 2014

1. Introduction

Reduction of greenhouse gas emissions is one of the most important challenges that the power industry will face in the next decades (IEA and UNIDO, 2011; Metz et al., 2005). Carbon capture and storage (CCS) technologies could cut by at least one order of magnitude the CO_2 emissions from fossil fuel-fired power plants. In all future energy scenarios aimed at carbon mitigation, CCS is expected to give a significant contribution (22% of the total abatement in 2035 according to IEA 450 scenario) (IEA, 2008), similar to that of renewables (21%) and much more relevant than nuclear (9%).

Novel concepts for CO_2 capture have been studied in recent years to improve the thermodynamic and economic performance of power plants with CO_2 capture. Chemical looping combustion (CLC) is a process known since 1950s. In 1954, Lewis and Gilliland (1954) patented an invention related to the production of pure CO_2, free of inert gases. However, only 30 years later Ishida et al. (1987) first proposed CLC as possible technique aiming at improving power plant efficiency. The chemical looping combustion concept is based on the indirect oxidation of a fuel by means of a solid metal which is alternatively oxidized and reduced by sequentially contacting the oxygen carrier (OC) with air and fuel. In such a way, dilution with nitrogen of the combustion products is avoided and the resulting exhaust gas is highly concentrated in CO_2. Extensive research has been carried out in the last 15 years on concept studies, on the properties and performance of a large number of oxygen carriers and on demonstrating continuous operation in lab-scale reactors, mainly using gaseous fuels. More recently, the direct utilization of coal in a CLC system has also been the object of relevant research efforts. The progress of the research in this field and the most relevant results obtained up to now have been recently extensively described by (Adanez et al., 2012). A review on the most relevant patents on CLC has been presented by Gallucci and van Sint Annaland (2011).

* Corresponding author. Tel.: +39 0223993846.
E-mail address: matteo.romano@polimi.it (M.C. Romano).

Nomenclature

AGR	acid gas removal
AR	air reactor
ASU	air separation unit
BOP	balance of plant
CCS	carbon capture and storage
CGE	cold gas efficiency, $Q_{LHV,syngas}/Q_{LHV,coal}$
CLC	chemical looping combustion
CLOU	chemical looping with oxygen uncoupling
FGD	flue gas desulfurizer
FR	fuel reactor
GT	gas turbine
HP-IP-LP	high-intermediate-low pressure
HR	heat removal phase
HRSC	heat recovery steam cycle
HRSG	heat recovery steam generator
HT-IT-LT	high-intermediate-low temperature
IC	inter-cooled
IGCC	integrated gasification combined cycle
IGCLC	integrated gasification chemical looping combustion
LHs	lock hoppers
LHV	lower heating value, MJ/kg
MDEA	methyl diethanolamine
NG	natural gas
OC	oxygen carrier
Ox	oxidation phase
PBR	packed bed reactor
Red	reduction phase
SC	steam cycle
SCOT	Shell Claus off-gas treating
SH/RH	superheated/reheated
SPECCA	specific primary energy consumptions for CO_2 avoided, MJ_{LHV}/kg_{CO_2}
ST	steam turbine
SWS	sour water stripper
TIT	turbine inlet temperature
TOT	turbine outlet temperature
TSA	temperature swing adsorption
USC	ultra supercritical
WGS	water gas shift

Symbols and abbreviations

c_p	specific heat J/kg K
E_{CO_2}	CO_2 specific emissions, kg_{CO_2}/MWh_e
m	mass flow rate, kg/s
m_{dl}	dimensionless mass flow rate, m_i/m_{syngas}
N	molar flow rate, kmol/s
P	pressure, bar
Q_{LHV}	thermal power, MW_{th}
t_{dl}	dimensionless time, t_i/t_{cycle}
t	time, s
T	temperature, °C
η_e	net electric efficiency

Most of the studies on CLC up to now considered the conversion of gaseous fuels in interconnected fluidized bed reactors (Fig. 1a), whose operability at atmospheric pressure has been demonstrated by different research groups at scales up to 3 MW_{th} (Abad et al., 2012; Andrus et al., 2009; Kolbitsch et al., 2010; Linderholm et al., 2012; Sit et al., 2012; Son and Kim, 2006). This means that these systems proved to be able to deliver hot gaseous product streams with stable temperature and flow rate at atmospheric pressure, allowing an intrinsic separation of the CO_2. Considering the results obtained in these lab-scale demonstration facilities, no major challenges are expected for continuous operation of industrial-scale CLC processes in interconnected circulating fluidized bed reactors at atmospheric pressure. On the contrary, major challenges are expected in operating pressurized CLC systems, due to the difficulties of maintaining a stable solids circulation between the reactors. This is a critical issue for the CLC technology, since high pressure operation is needed to integrate the CLC process in a gas turbine-based combined cycle, as required to increase plant efficiency. High-temperature, high-pressure gas filtration from OC particles, inevitably entrained from the fluidized bed reactors, before expansion in the gas turbine is another major challenge to be solved for the application of CLC using interconnected fluidized beds.

A different approach based on packed bed reactors (PBRs) has been proposed by Noorman et al. (2011) for CLC at pressurized conditions to overcome the hurdles posed by circulating fluidized bed reactors. In this case the solids remain stationary while the gaseous streams are switched to the different reactors that are operated alternatively in the oxidation (Ox) and reduction (Red) mode as depicted in Fig. 1b.

The operation of fixed bed reactors for CLC is intrinsically dynamic. It leads to the formation of a reaction front and a heat front, with different velocities.[1] Introducing dynamically operated PBRs in a power plant is possible because the reaction front is faster than the heat front: therefore the heat released during the oxidation reaction is retained in the bed at high temperature and a stream at constant high temperature and mass flow rate can be produced during a Heat Removal (HR) phase (Noorman et al., 2011; Spallina et al., 2013a). In order to avoid mixing of fuel and air during the reactors switch (for safety and for performance reasons), one or more purge phases are also required. While solving the major technical issues of pressurized fluidized beds (neither need of solid circulation nor high temperature particle filtration, assuming a proper mechanical resistance of the OC), PBR reactors show other relevant technical challenges: (i) the need of very high temperature valves and gas piping system, and (ii) the unsteadiness in temperature and flow rate of the streams exiting the reactors, that can be unsuitable for the downstream expander. To achieve a good stability of outlet gas conditions, proper heat management strategies need to be developed by considering the properties of the OC and the fuel used, since the kinetics of reduction is very sensitive to the solid temperature and gas composition.

The solid temperature profile at the beginning of each phase depends on the operation of the previous one. When a gaseous stream is fed to the reactor, the temperature of the initial part of the bed tends to be close to the inlet gas temperature because the solid is continuously in contact with a stream at constant (moderate) temperature. If the temperature of the inlet gas is not sufficiently high, the oxygen carrier will not react with a sufficiently fast kinetics with the gaseous stream in the subsequent phase and the process cannot proceed in a stable and continuous way.

In the case of an oxygen carrier showing both high reactivity at low temperature and resistance to high temperature operations (such as Ni/NiO), syngas oxidation can be carried out on a relatively cold reactor after the heat removal phase. Another option is employing two different oxygen carriers in the same reactor, as proposed by Hamers et al. (2013). In this case, a highly reactive Cu-based OC is used at the reactor inlet to initiate the syngas oxidation reaction, while Mn-based OC suitable for high temperature

[1] The reaction front divides the bed into two portions: the initial part (close to the reactant inlet) where the carrier has already reacted, and the final one filled with unreacted material. The heat front divides the bed into zones at different temperature.

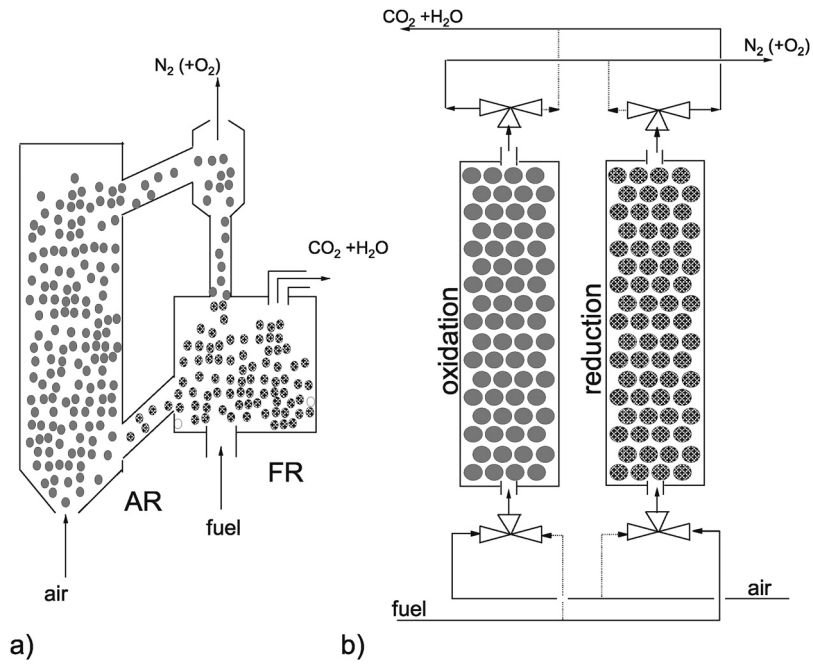

Fig. 1. Schematic representation of the CLC process with interconnected fluidized bed reactors (left) and parallel dynamically operated packed bed reactors.

operation is used in the second part of the bed to reach the high temperatures needed by the power cycle. A correct proportion between the two OC allows keeping the OC at temperatures high enough for fast kinetics but below their melting temperature.

A different approach has been proposed by Spallina et al. (2013a). In this case, ilmenite ($FeTiO_3$) has been selected as OC due to its low cost and stability at high temperature. Ilmenite shows very high selectivity to CO_2 and H_2O when reacting with syngas and very high temperature increase is achieved during the oxidation reaction from $FeTiO_3$ to $Fe_2TiO_5 + TiO_2$ (Leion et al., 2008). Differently from Fe-based oxygen carrier, where the Fe_2O_3/Fe_3O_4 pair is usually considered to avoid low selectivity to CO_2 and H_2O (Jerndal et al., 2006), in the case of ilmenite the interaction with titanium or alumina allows to further reduce the Fe_3O_4 to FeO and obtain full gas conversion (Leion et al., 2008). In order to improve the solid conversion with syngas (CO oxidation with ilmenite is very slow at temperatures below 750 °C) the reduction phase is carried out just after the oxidation is completed and the bed is at its highest temperature level. The heat stored in the bed at the end of the reduction phase is removed by a large N_2 stream, which is released at high temperature and pressure, producing power in a gas expander. This strategy was adopted in the present analysis and it will be further discussed in more detail in the next sections.

The aim of the present paper is to carry out a thermodynamic analysis of an integrated gasification power plant using dynamically operated packed bed reactors for chemical looping combustion. First, a review of different strategies for plant integration with CLC technology is presented both for coal and natural gas based power plants. The plant configuration assessed in this work is then discussed in detail, followed by a sensitivity analysis on the main process parameters. The comparison of the different systems is presented by evaluating and discussing their mass and thermal balances and their main performance indices. The performance of the CLC based systems resulting from the thermodynamic analysis are finally compared to benchmark processes and the main technological uncertainties are identified and discussed.

2. Integration of CLC in complete power plants

The general and simplest layout of a pressurized CLC power plant is based on a compressor, which feeds high pressure air to the air reactor (AR). Here, metal oxidation occurs by taking the oxygen from the inlet air stream while the depleted air stream exits the reactor at high temperature thanks to the reaction exothermicity. In fluidized bed based configurations, proper air excess is fed to the AR to limit the temperature to the maximum value acceptable for the OC. The high temperature and high pressure oxygen-depleted air is subsequently expanded in a turbine producing mechanical power. A clean gaseous fuel is fed to the fuel reactor (FR) where it is oxidized by the OC, producing a CO_2/H_2O stream undiluted with N_2, ready for CO_2 storage after cooling, water condensation and final compression. In other words, the CLC reactor system typically replaces the combustor of a gas turbine.

There is a strong incentive to increase the OC stability at high temperatures considering that the turbine inlet temperature (TIT) strongly affects the overall efficiency of a combined cycle. For temperatures above 1000 °C, the electric efficiency of natural gas fired CLC based plants is in the range of 47–53%, as shown by Consonni et al. (2006) and Naqvi and Bolland (2007). They calculated that a 100 °C TIT increment leads to a net electric efficiency gain of about 2 percentage points. Besides the TIT, the gas cycle pressure ratio is the other important cycle parameter, to be optimized according to the achievable TIT. Higher TITs and hence higher efficiencies can be obtained by adding a post-combustion on the AR exhaust (which has a proper O_2 residual content), while maintaining the oxygen carrier at lower temperature. Consonni et al. (2006) assessed a system including such a post-firing step, obtaining a net efficiency of 52.2% (+9 percentage points with respect to the 850 °C TIT, unfired case) by increasing the AR exhaust temperature from 850 °C to 1200 °C. However, since natural gas was used for post-firing, CO_2 emission increased accordingly from zero to 175 kg/MWh$_e$, lowering the carbon capture rate (CCR) from a virtual 100% to around 53%.

Another option to increase the average temperature of the heat introduction in the thermodynamic cycle (and hence its efficiency)

while maintaining acceptable temperatures of the solid material has been proposed by Naqvi and Bolland (2007). This approach is based on a reheated cycle, where two CLC units operating at different pressures are employed to produce a high temperature O_2-depleted air stream expanded in two turbines in series. Efficiencies higher than 53% have been reported in this study for a TIT of 1200 °C, with optimized pressures of the two CLC sections.

An alternative fired case was proposed by Lozza et al. (2006), where H_2-based decarbonized fuel is produced in a steam reactor where H_2O is reduced to H_2 by reacting it with FeO, afterwards further oxidized to Fe_3O_4 by reaction with air. This three-reactor CLC layout, also proposed for hydrogen production by Chiesa et al. (2008), allows the thermodynamic cycle to operate at 1350 °C without any additional CO_2 emissions with an electrical efficiency in the range of 50.2–51.3%.

Finally, a layout based on a regenerative humid air gas turbine cycle (HAT) was proposed in early works on CLC technology (Brandvoll and Bolland, 2004; Ishida and Jin, 1994). Despite the highest net electric efficiency reported of 55.9%, the configuration proposed contains some components unusual for large scale commercial power plants (i.e. highly intercooled air compression and recuperative cycle) that make the economic advantage doubtful when compared to the conventional combined cycle configuration.

Different layouts have been proposed to recover the heat from the CO_2-rich stream produced in the FR. Hot, high pressure CO_2-rich stream can be either cooled in a pressurized heat recovery steam generator (Consonni et al., 2006; Ishida and Jin, 1994; Wolf et al., 2005) or expanded in a CO_2/H_2O expander down to nearly atmospheric pressure before cooling, water separation and CO_2 recompression (Naqvi et al., 2007).

The use of coal as primary fuel in a CLC-based power plant can be accomplished by two different conceptual layouts. In the first case, coal is initially converted into a gaseous fuel in a gasification process and, after heat recovery and acid gas removal, the syngas is used as fuel of the CLC unit. The second option is the direct coal oxidization in the fuel reactor of a CLC system performed in steam cooled reactors operating at atmospheric pressure. In this case, heat released in the CLC unit is supplied to a steam cycle.

The first configuration has been studied by Erlach et al. (2011), who considered pressurized reactors (20 bar) and assessed two different options for CO_2-rich stream cooling (expansion followed by steam generation and steam generation only). The analysis discusses also the performance at different maximum CLC solid temperatures, obtaining a +1% point of net electric efficiency increase by increasing the maximum temperature from 1200 °C to 1300 °C under optimized maximum steam cycle pressures. A similar study has been proposed also by Rezvani et al. (2009), who proposed two plant configurations. In the first case only one CLC unit working at 20 bar and 1200 °C is considered (with a TIT equal to 1074 °C), obtaining a net electric efficiency of 34.5–35.2%. In the second case, two CLC pressure levels are considered (at 20 bar and 7 bar) to sustain a reheated gas cycle and obtaining an efficiency of 36.1%.

A preliminary comparison of combined cycle and ultra-supercritical steam cycle adopting CLC from coal syngas with PBRs has been presented in Spallina et al. (2013b). The analysis showed that the first configuration achieves an electric efficiency three percentage points higher (40 vs. 36.9%) when a 1200 °C maximum reactor temperature is considered. On the other hand the efficiency of the second configuration is almost independent of the pressure and temperature of the CLC system. Nevertheless, a low pressurization level (below 5–10 bar) leads to economically unacceptable reactor cross sections when adiabatic reactors are considered. Heat removal by steam generation directly inside the PBRs (that could reduce the footprint of the reactors) would in turn make the reactor design much more complex and would entail local cooling that inhibits the kinetics. For these reasons, ultra-supercritical steam cycles are not assessed in the present paper that, on the contrary, includes a deeper analysis of the CLC based combined cycle configuration.

Sorgenfrei and Tsatsaronis (2014) discussed an IGCC power plant with iron-based syngas for CLC similar to the work discussed by Lozza et al. (2006) for natural gas fired power plant. Two different gasification technologies (Shell and BGL) have been considered in the paper. Electric efficiencies in the range of 39.7–44.8% are reported for plants featuring hot gas desulfurization operated at 550 °C.

3. Packed bed reactors for CLC

The CLC cycle in dynamically operated packed bed reactors consists of consecutive oxidation, reduction and heat removal phases. It was studied and described using a 1D adiabatic packed bed reactor model, as discussed by Spallina et al. (2013a) for a demo-scale reactor working with syngas from a coal gasification plant. In this section, the methodology and the assumptions used for simulating the CLC unit are summarized to better define the link between the dynamic PBR system and the power plant, which is supposed to be operated at nearly steady state conditions. A comprehensive analysis of the effects of the design and operating strategy of the CLC reactors is beyond the scope of this work and will be addressed in a future work. However, it can be anticipated that different reactors operating in parallel are needed during each one of the main phases (oxidation, reduction and heat removal). It is hence possible to stabilize the temperature of the mixed stream fed to the downstream equipment (turbine and heat exchangers) by simply running the reactors of each phase with a proper time lag. Following the results obtained in (Spallina et al., 2013a), the heat management strategy selected for the plant is here briefly summarized. It entails that the reactors are operated sequentially in oxidation/purge/reduction/heat removal phases, so that the OC reduction occurs just after oxidation at the maximum bed temperature in order to have proper reduction reaction rates, while an inert gas (N_2) is used during the HR stage on the reduced OC. Two different configurations have been studied in the analysis:

a) Co-current feeding (Fig. 2a): all the streams are fed to the same reactor end. In this case the CO_2/H_2O stream is released mostly at the highest temperature (around 1200 °C in the specific case) because it is heated up by flowing across the hot portion of the bed (note in Fig. 2c the temperature profile after the oxidation phase).
b) Counter-current feeding (Fig. 3a): during the oxidation phase, the air stream is fed to the opposite bed end with respect to the streams fed during the other phases. In this configuration, CO_2/H_2O stream is produced at a lower average temperature, as a consequence of the bed temperature profile resulting from the oxidation phase, leaving the top end of the reactor at the temperature of the air coming from the compressor (400/450 °C). Correspondingly, a higher fraction of the heat is stored in the bed after oxygen carrier reduction and is released at high temperature to the N_2 stream in the heat removal phase, leading to a potentially higher plant efficiency. A major drawback of this configuration is that high temperature valves and piping are required at both the ends of the reactors.

The 1-D analysis was helpful to study and quantify the behavior, the operating limitations and the time-dependent conditions of the gas streams produced by the PBRs unit of a full scale power plant. Average values evaluated from the 1-D simulation have then been used to describe the behavior of the CLC system in the

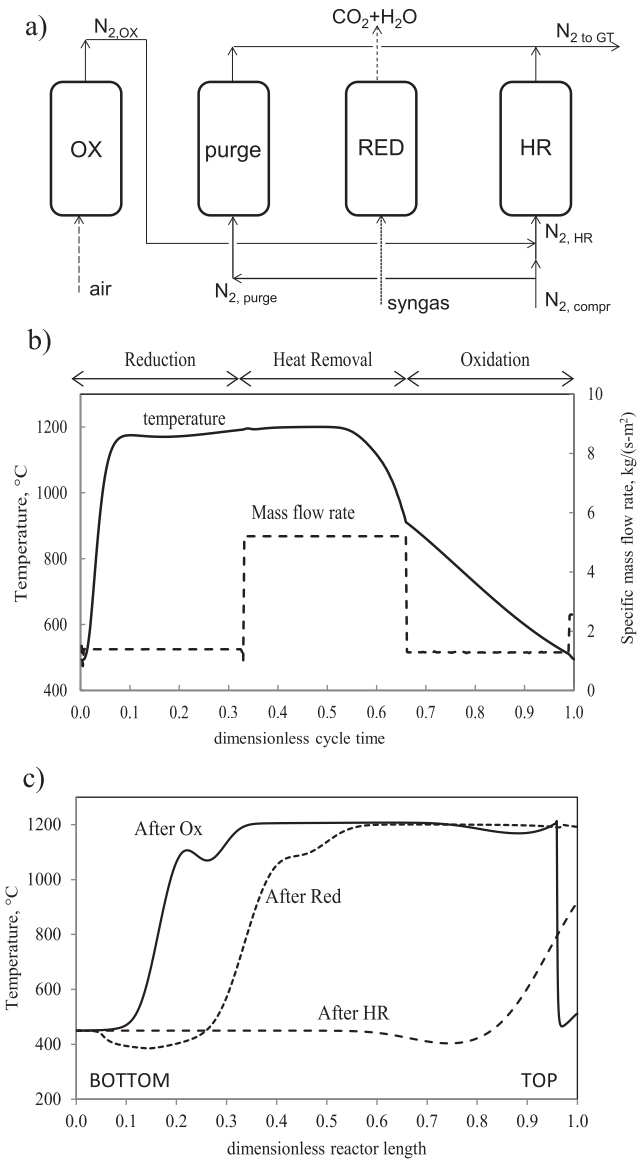

Fig. 2. Schematic of the co-current configuration (a), gas conditions at the reactor outlet (b) and solid temperature profile of the reactor after the oxidation/reduction/heat removal phases (c) as described in Spallina et al. (2013a).

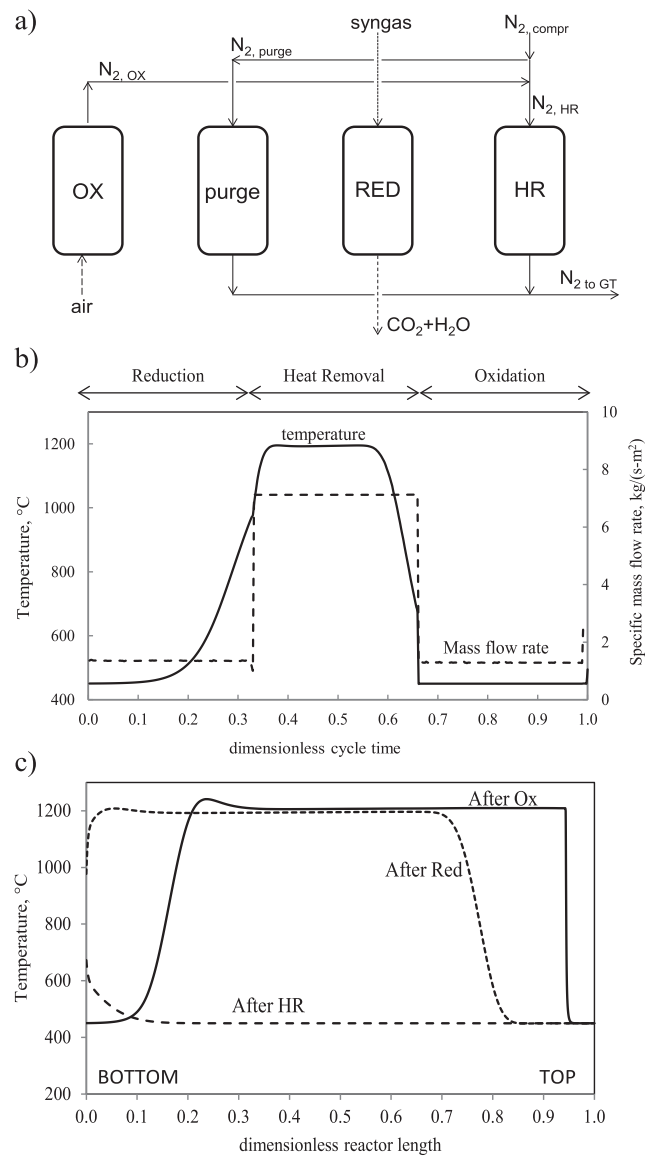

Fig. 3. Schematic of the counter-current configuration (a), gas conditions at the reactor outlet (b) and solid temperature profile of the reactor after the oxidation/reduction/heat removal phases (c) as described in Spallina et al. (2013a).

Table 1
Main assumptions used for the adiabatic 1D model.

Packed bed reactors (from 1D model)	
Active weight content – OX, wt.% of FeO[a]	27.8–31.7
Active weight content – RED, wt.% of Fe_2O_3[a]	30.0–34.0
Particle diameter, mm	5
Reactor void fraction	0.4
Reactor length, m	11
Reactor diameter, m	5.5
Maximum reactor pressure drops, $\Delta p/p$	0.08
Purge gas mass flow rate, kg/s	30
Maximum solid temperature, °C	1200

[a] The range of values used in this work is reported. The actual value depends on the temperature of the N_2 used for the HR phase and hence changes with the pressure ratio of the gas cycle.

steady-state process simulation software employed to perform the heat and material balances of the power plant.

The set of assumptions used for the 1-D calculations of the PBRs of the large scale power plant are reported in Table 1. The active weight content of the oxygen carrier was selected to limit the maximum temperature during the oxidation phase to 1200 °C.

4. Power plant description

The general power plant layout considered in this study originates from the full integration of the following 4 main sections (Fig. 4):

- Syngas production and cleaning: in this unit, coal is gasified and the resulting syngas is cleaned from sulfur and other contaminants with conventional low temperature processes. As a result a clean H_2/CO-rich syngas is produced at high pressure;
- CLC island: in this unit syngas fuel is converted into CO_2 and H_2O; high pressure, high temperature N_2 is generated for the gas turbine as described in the previous section;
- Power island: the power production is carried out in a combined cycle type unit which is based on Joule-Brayton thermodynamic cycle operated by a semi-closed gas turbine cycle using N_2 as

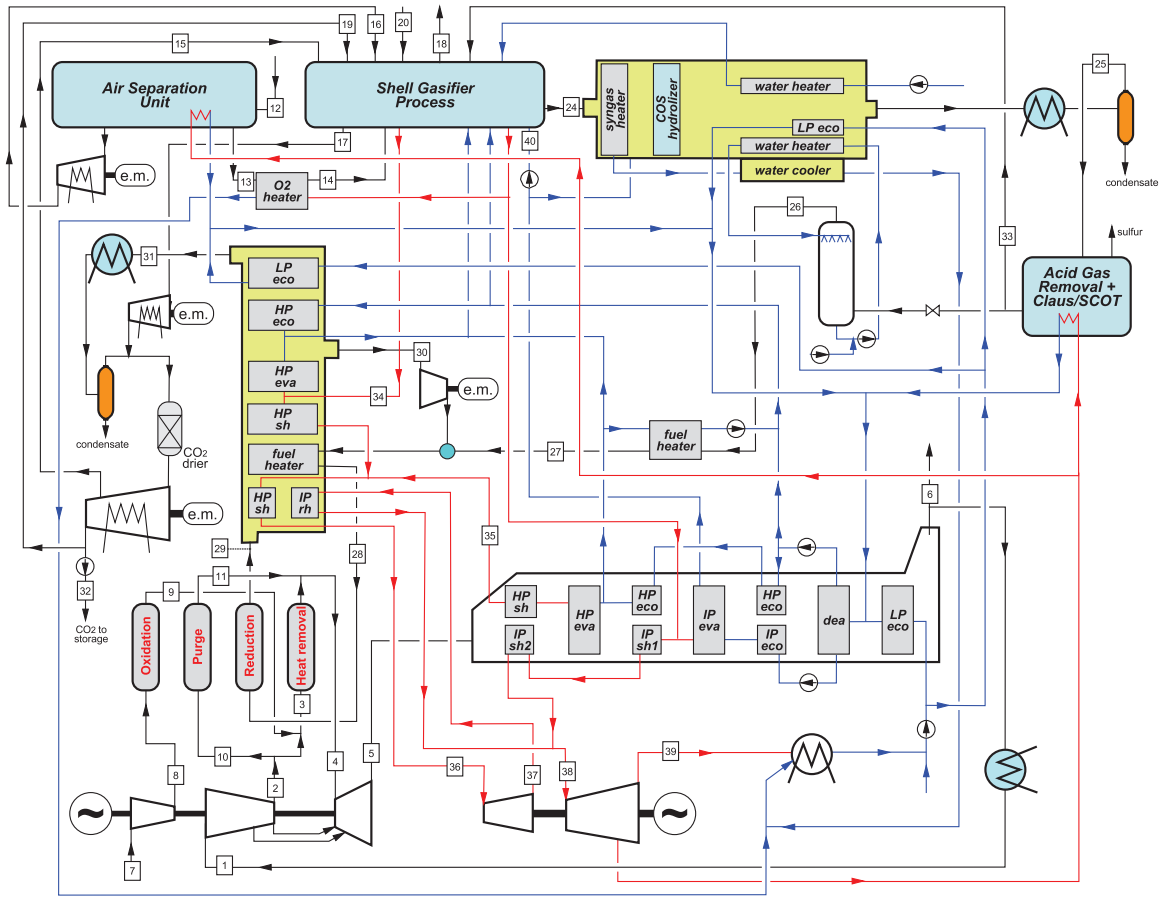

Fig. 4. Detailed layout of the IGCLC plant, with PBRs co-current feeding system and HT CO_2/H_2O stream.

main working fluid. In addition to the main N_2 compressor and expander, a smaller air compressor is also used to provide fresh stoichiometric air for oxidation. The steam raised at different pressure by cooling the hot streams of the plant produces additional electricity in a highly integrated heat recovery cycle.

- CO_2 treating unit: in this part of the plant the pressurized CO_2/H_2O stream from the CLC unit, after a proper heat recovery process, is cooled to nearly ambient temperature, dried and compressed to produce a high purity CO_2 stream for long-term storage.

Simulations have been carried out by the proprietary computer code GS (Gecos, 2013) developed by the GECOS group at the Department of Energy of Politecnico di Milano. The calculation code is designed according to a modular structure allowing to calculate complex plant configurations. Among the components available in the code (e.g. compressor, expander, splitter, mixer, heat exchanger, combustor, pump) the gas turbine model deserves particular attention, because it is able to simulate a cooled expansion on the basis of a one-dimensional design of the turbine stages for an accurate estimation of the cooling flows for each row as described in Chiesa and Macchi (2004). Since this model is based on general correlations whose validity is independent of the working fluid properties, it can reliably predict the behavior of the N_2 turbine included in the plants considered in this study. The CO_2 compression unit is calculated by using Aspen Plus 7.3 (Aspen Technology, 2011), adopting the Peng–Robinson equation of state with default coefficients for the evaluation of the fluid mixture properties. AGR and ASU units were not calculated in this work, but specific electric and thermal consumptions are taken from (EBTF, 2011) and (IEAGHG, 2005) respectively.

4.1. Gasification and syngas cleaning

The entrained flow, oxygen blown, dry feed Shell-type gasification process represented in Fig. 5 is used in the plant. Coal (stream #20) is pulverized and dried by burning some sulfur-free syngas (#33). The dried coal is then fed to the gasifier, operating at 44 bar, by using pure CO_2 as carrier gas in the lock hoppers (#15) instead of N_2 as usual in dry feed gasifiers for IGCC plants to avoid excessive dilution of the final CO_2. Part of the CO_2 released from the lock-hoppers is recovered, re-compressed and fed to the CO_2 treating unit to reduce CO_2 emissions (#17). Part of N_2 from the ASU (#16) is also used in the lock hoppers (around 10% of the total amount of gas required) and then vented in the atmosphere with the remainder CO_2 (#18). The gasifier is a slagging reactor, with membrane walls cooled with 54 bar boiling water (#40). The system is characterized by high carbon conversion (>99%) and cold gas efficiency (around 80%). High purity (95% vol.) oxygen (#13) is produced in a stand-alone, dual-reboiler low-pressure cryogenic air separation unit (ASU), whose specific consumptions have been assumed according to (IEAGHG, 2005). The O_2 stream is pumped in liquid phase to the required pressure inside the ASU and fed to the gasifier after heating to 180 °C (#14) by condensing IP steam. The hot syngas at the gasifier outlet is quenched to 900 °C (#21) with low temperature recirculated syngas (#23) taken partly after the LT syngas cooler and partly after the scrubbing unit. Data on syngas composition at point #21 (after mixing with recycle quench

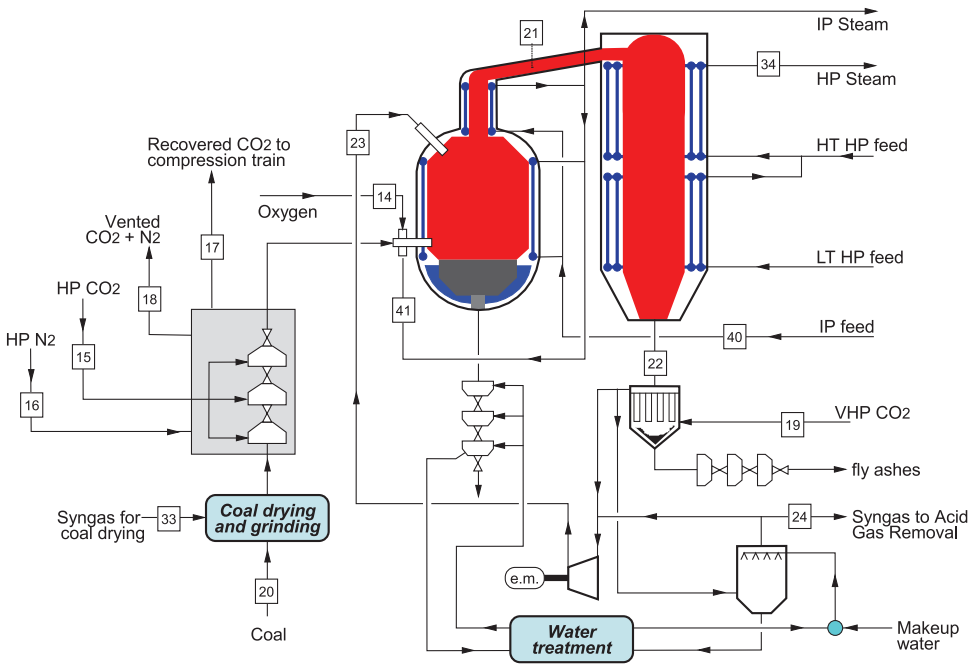

Fig. 5. Schematic of the Shell gasification unit.

stream #23) provided by the industrial partners of the Democlock project (Democlock, 2011–2015) were used to calibrate the gasifier model.

At 900 °C the molten fly ashes entrained by the syngas solidify and the product stream is first cooled down to 300 °C in a convective heat exchange section by producing superheated (400 °C) HP steam (#34), and then washed in a wet scrubber unit that removes residual solids and soluble contaminants.

In order to enhance the sulfur removal from the scrubbed syngas stream (#24), COS is hydrolyzed to H_2S in a fixed bed reactor operating at 180 °C. The syngas is subsequently cooled down to ambient temperature and sent to the AGR section. Here, H_2S is removed from syngas by washing with selective solvents in an absorption tower operating at high pressure and low temperature. A Selexol physical absorption process, using dimethyl ether of polyethylene glycol as solvent, has been assumed for evaluation of the plant thermal balance. Sulfur removal efficiency exceeds 99% and the heat for the reboiler of the regenerator is provided by condensing LP stream. Sulfur recovery is completed in a Claus plant where H_2S is converted to elemental sulfur. Claus plant tail gas, still rich in sulfur compounds, is afterwards treated in a SCOT unit, where the residual sulfur species are catalytically converted back to H_2S and recycled to the absorption column of the AGR unit.

After sulfur removal, the clean syngas is heated up and saturated with hot water in a saturator (#26) and further heated to 300 °C (#27) by cooling HP saturated water before feeding it to the CLC unit. In order to achieve the desired inlet temperature and a proper syngas dilution to avoid carbon deposition and iron oxide over-reduction, the clean syngas is first mixed with recirculated exhaust gas (#30). The resulting diluted syngas ($CO_2 + H_2O$ fraction is higher than 50% on molar basis) is heated to the desired temperature with the CO_2-rich stream leaving the CLC unit at high temperature. A different approach for syngas humidification and pre-heating was considered in (Spallina et al., 2013b), where a high temperature recycle of the CO_2/H_2O stream directly taken at the reduction reactor outlet was proposed. In this case, the high temperature of the stream prevented the application of a fan in order to overcome the pressure drop of the recirculated flow. Hence, an ejector was used, to entrain the high temperature recirculated flow by means of the high pressure syngas stream. This solution was not considered in this analysis because of the unusual operating conditions and possible control problems. Table 2 finally summarizes the main assumptions used for the simulation of the gasification section.

4.2. Gas turbine and HRSC

The integrated gasification plant with chemical looping combustion (IGCLC) includes a combined cycle for power generation. Conventional combined cycles are based on a gas turbine where the air required for the combustion (in large excess compared to the stoichiometric ratio to limit the cycle peak temperature) is compressed by a single compressor and the reaction products are expanded in a turbine. As anticipated, in this case the power section is based on a semi-closed gas turbine cycle using nitrogen as working fluid. As shown in Fig. 4, the recirculated N_2 stream from the HRSG outlet (#1) at nearly ambient pressure is compressed and mixed with a minor N_2 flow exiting the oxidation reactor (#9). A supplementary air compressor supplies the air stream required for the CLC oxidation phase (#8). As a small fraction of the N_2 stream is used for the purge phase (#10), most of the N_2 stream receives heat from the CLC system during the heat removal step, increasing its temperature. The hot nitrogen stream is then expanded in the gas turbine (#4), whose inlet temperature is set equal to the maximum allowable temperature assumed for the solids in the PBR (about 1200 °C), which is significantly lower than the peak temperature tolerated in modern commercial units.

The gas turbine is calculated to reproduce the performance of an advanced state-of-the-art industrial heavy duty machine, currently used in large scale natural gas-fired combined cycle power plants. The gas turbine N_2 exhaust stream is cooled down in a double pressure with reheat heat recovery steam generator. Due to the large amount of steam generated in the other heat recovery sections (syngas coolers and CO_2/H_2O stream coolers) and pre-heated in the HRSG, a low pressure level is not required for a proper cooling of the exhaust nitrogen. In addition, depending on the temperature of the CO_2/H_2O stream generated in the CLC unit, final SH and RH tube banks can be placed in different sections of the plant and different

Table 2
Set of assumptions for the simulation of the syngas production and purification unit.

Bituminous South African coal (composition and heating values)	
Composition, wt.%: C 66.52 (fixed C 54.9%); N 1.56; H 3.78; S 0.52; O 5.46, ash 14.15; moisture 8.00.	
LHV: 25.02 MJ/kg; HHV: 26.04 MJ/kg	
Gasification and coal pre-treating unit	
Gasification pressure, bar	44
Oxygen to carbon ratio, kg_{O_2}/kg_{coal}	0.903
Heat losses in gasifier, % of input LHV	0.7
H_2O in coal after drying, % wt.	2
Fixed carbon conversion, %	99.3
Moderator steam, kg_{H_2O}/kg_{coal}	0.09
Moderator steam pressure, bar	54
Oxygen pressure, bar	48
Temperature of O_2 to gasifier, °C	180
Heat to membrane walls, % of input coal LHV	2
Slag handling, kJ_e/kg_{ash}	100
Syngas quench	
Quenched syngas temperature, °C	900
Cold recycled syngas temp, °C	300
Recycle compressor polytropic efficiency, %	75
Recycle compressor el./mech. efficiency, %	92
CO_2 operated lock hoppers	
VHP/HP CO_2 pressure, bar	88/56
CO_2 temperature, °C	80
CO_2 consumption, $kg_{CO_2}/kg_{dry\text{-}coal}$	0.826
Electric consumption for coal milling and handling, kJ_e/kg_{coal}	50
CO_2 not recovered for CCS, % of CO_2 inlet flow rate	10
Air separation unit	
Oxygen purity, mol%	95
Pressure of delivered oxygen, bar	48
Pressure of delivered nitrogen, bar	1.2
Temperature of delivered O_2 and N_2, °C	22
Electric consumption, kWh_e/t_{O_2}	325
LP steam heat rate for TSA beds regeneration, kWh_{th}/t_{O_2}	58.3
Heat exchangers	
Minimum ΔT in liquid–liquid heat exchangers, °C	10
Minimum ΔT in gas–liquid heat exchangers, °C	10
Minimum ΔT in gas–gas, °C	25
Minimum ΔT in condensing fluid–liquid heat exchangers, °C	3
Heat losses, % of heat transferred	0.7
Gas side Pressure drop, %	2
Maximum steam T in the syngas coolers, °C	400
Acid gas removal (Selexol process)	
Syngas temperature at absorption tower inlet, °C	35
Syngas pressure loss, %	1
Heat duty from LP steam, MJ_{th}/kg_{H_2S}	20.95
Electric consumption, MJ_e/kg_{H_2S}	1.93
Others	
Miscellaneous BOP, % of input coal LHV	0.15
Overall pressure losses before PBR, %	11

maximum steam temperatures can be correspondingly achieved, as discussed in the following section.

The steam flows generated in the different plant sections (#36 and #38) are expanded in the steam turbine. The main design parameter assumed for the gas turbine and heat recovery steam cycle (HRSC) are listed in the Table 3. Some of the assumptions (compressor pressure ratio and steam cycle pressures) are varied in the sensitivity analysis to evaluate their effect on the global plant performance.

4.3. Exhaust cooling and CO_2 compression

The exhaust gases leaving the reactor operated in the reduction phase (#29) are produced at high pressure and high temperature. They must be cooled to recover heat and to condense water, producing a high purity CO_2 stream. Two configurations were adopted for the heat recovery process. In the case of HT exhaust gases (1156 °C), produced by the co-current reactors feeding (Fig. 2), heat is most efficiently recovered by superheating and reheating steam, up to the maximum assumed temperature of 565 °C, as shown in Fig. 4. The additional heat available at low temperature is used for CLC fuel heating, HP steam generation and HP economizer. This highly interconnected configuration enables a high efficiency, but requires a broader use of HT pipes and headers to manage the superheated steam generated in different plant sections.

In the case of counter-current reactors feeding (Fig. 3), exhaust gases are released at an average temperature of 482 °C, too low for superheating/reheating. Heat is used for syngas heating, for production of saturated HP steam (superheated afterwards by the gas turbine exhausts) and for HP economizer. In this layout, a considerable simplification is expected for the steam piping network.

After water condensation and further drying (to reach a water content below 50 ppm), a CO_2 purity of 96.5% is achieved with mainly N_2 and Ar impurities originating from the high purity O_2 produced in the ASU and from the nitrogen in the primary feedstock. This stream, which is considered sufficiently pure for CCS applications, is compressed in a three-stage intercooled compressor up to 88 bar, liquefied at 23 °C and finally pumped to 110 bar (#32). Assumptions for the calculation of the CO_2 treating and compression unit are resumed in Table 4.

Table 3
Set of assumptions for the simulation of the power island. For compressor pressure ratio and steam cycle pressure levels, the ranges investigated in the sensitivity analysis are reported.

N_2 gas turbine	
Compressor inlet pressure, bar	1.01
Compressor pressure ratio	11–23
Maximum compressor polytropic efficiency[a], %	92.5
Maximum efficiency of large turbine stages (cooled/uncooled)[a], %	92.1/93.1
Gas turbine auxiliaries consumption, %	0.35
Mechanical efficiency of compressor/turbine, %	99.865
Electric generator efficiency, %	98.7
Air compressor	
Compressor pressure ratio	11.5–24.1
Maximum compressor polytropic efficiency[a], %	92.5
Heat recovery steam generator	
Gas side pressure loss, kPa	3
Heat losses, % of heat transferred	0.7
HP pressure level, bar	120–170
IP pressure level, bar	20–54
Maximum SH/RH steam temperature, °C	565
Minimum approach point ΔT, °C	25
Pinch point ΔT, °C	10
Sub-cooling ΔT, °C	5
Pressure losses in HP/LP economizers, %	25
Pressure losses in superheaters/reheaters, %	7/8
Steam cycle	
Condensing pressure, bar	0.048
HP/IP/LP pumps hydraulic efficiency, %	85/75/85
HP/IP/LP steam turbine isentropic efficiency, %	92/94/88
Turbine mechanical efficiency, %	99.6
Electric generator efficiency, %	98.5
Power for heat rejection to the environment, MJ_e/MJ_{th}	0.008

[a] Values in the table are referred to large machines: the actual efficiency is calculated by GS code as function of the machine/stage size.

5. Results

5.1. Benchmark IGCC plants with and without CO_2 capture

The reference plant without CO_2 capture is an IGCC based on the same gasification island of the IGCLC plants. The only

Table 4
Set of assumptions for the simulation of the CO_2 treating and compression unit.

CO_2 compression	
IC compressor isentropic efficiency, %	82
IC compressor mechanical efficiency, %	94
Last stage IC compressor CO_2 discharge pressure, bar	88
Inter-coolers outlet temperature, °C	30
Pressure drop in each intercooler, %	1
Pump mechanical efficiency, %	92
Pump hydraulic efficiency, %	75
CO_2 delivery pressure, bar	110
CO_2 condensation temperature, °C	23

difference is that a conventional N_2 coal loading system is used, instead of a CO_2-based one. The clean syngas is saturated, pre-heated and mixed with N_2 from the ASU, before being sent to the combustor of the combined cycle gas turbine. Two gas turbine technology scenarios have been considered in the analysis. The first one, named "advanced" and derived from the EBTF assumptions (EBTF, 2011) has a TIT of 1360 °C, in line with the state-of-the-art, natural gas-fired commercial machines available on the market. This scenario assumes that the current technological development is fully incorporated in gas turbines specifically designed to run on H_2-rich fuel. In the second scenario, named "current", more conservative turbine inlet temperatures of 1305 °C and 1261 °C has been assumed for the cases without and with CO_2 capture respectively, in line to values today adopted for machines designed for natural gas operation and derated to be adapted for syngas and hydrogen utilization.

The reference IGCC with pre-combustion CO_2 capture is based on the reference no-capture configuration, but it includes WGS reactors and a CO_2 removal unit based on physical absorption by the Selexol® process (IGCC-Sel). The WGS reaction is carried out after scrubbing and IP steam addition, with two reactors operating at different temperatures, to combine a high H_2 yield in the cold stage with fast kinetics and efficient high temperature heat recovery in the hot stage. After acid gas removal by the Selexol® process, featuring two absorption columns for sequential separation of H_2S and CO_2, H_2-rich gas is humidified, pre-heated and mixed with N_2 from ASU before combustion in the GT combustor.

The main efficiency penalty of the IGCC with CO_2 capture is associated to CO_2 separation and compression, responsible for a net electric efficiency loss of 3.7 percentage points. Another very important efficiency decay is associated to the steam addition to syngas before the WGS reactors. IP steam extraction brings about a reduction of the steam turbine power output accounting for an efficiency loss of 2.8 percentage points on the overall balance. The remaining efficiency loss is due to the lower CGE (72.8% respect to 81.1%) caused by the exothermic WGS reaction that correspondingly reduces the gas turbine power output at a given coal input.

The above power plants are compared by means of the typical performance indices usually defined for CCS power plants. In addition to the electric efficiency and the specific CO_2 emission, the specific primary energy consumptions for CO_2 avoided (SPECCA) is used (Eq. (1)) for performance assessment:

$$\mathrm{SPECCA} = \frac{(1/\eta_{el}) - (1/\eta_{el,ref})}{E_{CO_2,ref} - E_{CO_2}} \cdot 3600 \quad (1)$$

Due to the different benchmark technologies, the SPECCA coefficient has been evaluated for the system proposed referred to both the current available technologies ($\mathrm{SPECCA_{CUR}}$) and the advanced one ($\mathrm{SPECCA_{ADV}}$).

5.2. IGCLC configurations

The performance of the IGCLC operated in both co-current and counter-current configuration are reported in Table 5 together with the benchmark IGCC plants. For the reference case with co-current feeding (5th column in the Table 5), a net electric efficiency of 40.5% has been obtained, between 3 and 5 percentage points higher than the reference IGCCs with CO_2 separation by physical absorption, depending on the gas turbine technology scenario considered. Most of the power is generated by the steam turbine, which produces about 59% of the gross power, vs. 41% produced by the gas cycle (including both the air and the N_2 main compressors). Such a power share is significantly different from that of the reference IGCCs, where the gas turbine always contributes by about 60–64% of the gross power. This difference is related to the lower TIT of the gas turbine of the IGCLC plant, and to the absence of the expansion of the fuel oxidation products, which are formed during the reduction phase and therefore not fed to the gas turbine expander. The resulting plant gross efficiency is about 48.2%, which is an intermediate value with respect to the reference IGCCs with CO_2 capture (47.3 and 49.4% for the current and the advanced turbine cases respectively).

As far as auxiliaries are concerned, most of the consumptions are associated to O_2 production in the ASU, bringing about an efficiency decay of almost 4 percentage points. The second most important contribution is related to CO_2 compression, which accounts for a net efficiency decay of 1.8 (including the consumption for the partial recovery of the CO_2 released from the lock hoppers). Such a penalty is however significantly lower than for the CO_2 separation in the AGR unit and compression in the reference IGCCs (3.8 percentage points decay) and highlights the advantage of this CLC system, which intrinsically produces a concentrated CO_2 stream at high pressure. Another relevant efficiency penalty in IGCC plants is associated to N_2 compression (for both lock hoppers and, mainly, for syngas dilution before combustion), accounting for 3–5 percentage points of efficiency decay.

The IGCLC plant with CLC counter-current feeding (6th column in the Table 5), shows very similar performance, with a net electric efficiency of 40.5%. This value results from very similar gross efficiency and auxiliary consumption of the co-current case. However, the power share between gas and steam cycles is significantly different in this case, with the gas cycle generating about 55% of the total gross power. This result is due to the higher amount of heat available during the heat removal stage, as a consequence of the lower temperature of the CO_2/H_2O stream released from the CLC process.

Further improvement of the plant efficiency could have been obtained by adding a syngas expander to recover the pressure energy lost when throttling the syngas from the pressure at the outlet of the gasification island to the CLC unit pressure. It is estimated that an efficiency increase of around 0.5 percentage points could be achieved by including a syngas expander. However, such a configuration requires an additional turbo-expander and a rather complex heat exchanger network for syngas reheating after expansion. In addition, syngas expanders are typically not proposed by manufacturers for conventional IGCCs based on Shell gasifiers, where the energy associated with the pressure difference between the gasification island and the gas turbine combustor could also be recovered. Therefore, this option was not considered further in this study.

In addition to such promising electric efficiencies, IGCLC plants also feature extremely high CO_2 capture efficiencies of about 96%. In the assessed process, most of the CO_2 is emitted from the lock hopper system (72%, the remaining fraction being emitted by the syngas combustion for coal drying), while the CLC process allows a virtually complete CO_2 capture from fuel oxidation. Even lower emissions would hence be possible if the CO_2 recovery from the lock hoppers could be further optimized. As a result of the high efficiency and the high carbon capture, specific emissions of 33.9 g/kWh (about one-third of the reference IGCCs with

Table 5
Power balances of CLC power plants and benchmark IGCC plants with and without CO_2 capture.

Configuration Name	Units	IGCC	IGCC	IGCC	IGCC	IG-CLC	IG-CLC	IG-CLC	IG-CLC
CO_2 capture technology		-	-	Selexol®	Selexol®	CLC	CLC	CLC 20 bar	CLC 14 bar
State-of-the-art technology/configuration		Current	Advanced	Current	Advanced	Co-current	Counter current	Co-current best	Counter-current best
Gas turbine									
Compressor	MW_e	−228.3	−212.7	−241.7	−237.6	−208.4	−307.0	−240.2	−260.0
Air compressor (only CLC)	MW_e	–	–	–	–	−75.36	−74.25	−80.66	−66.93
GT expander	MW_e	494.3	527.5	510.0	565.4	455.5	609.7	499.0	545.8
Auxiliaries and generator losses	MW_e	−4.38	−5.18	−4.41	−5.39	−2.83	−3.76	−2.98	−3.60
Steam cycle									
Gross power	MW_e	179.5	194.6	161.2	184.8	242.5	185.7	239.8	197.6
Pumps	MW_e	−2.90	−3.49	−3.64	−4.10	−4.28	−3.59	−4.88	−3.69
Gasification island									
Air separation unit	MW_e	−29.56	−32.11	−32.69	−37.36	−33.85	−33.85	−33.85	−33.85
Syngas recycle fan	MW_e	−0.98	−1.08	−1.09	−1.24	−1.00	−1.00	−1.00	−1.00
Coal milling	MW_e	−1.52	−1.66	−1.69	−1.93	−1.60	−1.60	−1.60	−1.60
Ash handling	MW_e	−0.46	−0.50	−0.51	−0.58	−0.48	−0.48	−0.48	−0.48
Acid gas removal	MW_e	−0.35	−0.37	−14.72	−16.82	−0.37	−0.37	−0.37	−0.37
N_2 compressors[a]	MW_e	−34.14	−43.66	−29.75	−31.20	−1.36	−1.36	−1.36	−1.36
PBR auxiliaries	MW_e	–	–	–	–	−1.21	−1.21	−1.21	−1.21
CO_2 treating system									
CO_2 compression	MW_e	–	–	−19.66	−22.50	−12.48	−12.48	−11.01	−14.31
CO_2 LHs recovery	MW_e	–	–	–	–	−3.08	−3.10	−3.10	−2.83
Heat rejection auxiliaries	MW_e	−2.64	−2.70	−2.70	−2.94	−4.21	−4.18	−4.18	−4.17
Balance of plant	MW_e	−1.22	−1.32	−1.35	−1.54	−1.28	−1.28	−1.28	−1.28
Overall gross power	MW_e	441.1	504.2	425.1	507.3	411.4	410.3	414.9	413.0
Overall net power	MW_e	367.4	417.3	317.3	387.1	346.2	345.8	350.5	346.8
Coal thermal input, MW_{LHV}	MW_{th}	812.5	882.4	898.8	1026.9	853.9	853.9	853.9	853.9
Gross electric efficiency	%	54.29	57.14	47.30	49.40	48.18	48.05	48.59	48.36
Net electric efficiency	%	45.21	47.29	35.31	37.70	40.55	40.50	41.05	40.61
Cold gas efficiency	%	81.61	81.71	73.21	73.32	80.65	80.65	80.65	80.65
Carbon capture rate	%	–	–	93.0	93.0	96.1	96.1	96.1	96.1
CO_2 avoided (ref to $IGCC_{cur}$)	%	–	–	86.2	87.0	95.4	95.4	95.5	95.4
CO_2 specific emissions	kg_{CO2}/MWh_e	769.8	736.0	101.4	96.0	33.9	33.9	33.4	33.8
$SPECCA_{CUR}$	MJ_{LHV}/kg_{CO_2}	–	–	3.34	–	1.25	1.26	1.10	1.23
$SPECCA_{ADV}$	MJ_{LHV}/kg_{CO_2}	–	–	–	3.03	1.80	1.82	1.65	1.78

[a] The N_2 compressors include the consumptions for the N_2 used for coal loading in the lock hoppers and N_2 that is used for the syngas dilution before the combustor (only in the IGCCs).

CO_2 capture) are obtained, resulting in lower SPECCA coefficients ($1.2 - 1.8$ MJ_{LHV}/kg_{CO_2} depending on the benchmark technologies).

As far as CO_2 purity is concerned, purities higher than 96% (molar basis) are obtained. Most of the impurities are associated to N_2 and Ar in the high purity oxygen used for gasification, to nitrogen in the fuel and, for a minor part, to unconverted H_2 (0.03% mol basis) and CO (0.16% mol basis) in the CLC section. While such purity can be considered sufficiently high for some storage sites like aquifers, higher purities might be required for some other cases. The easiest option to increase CO_2 purity with a limited impact on the process would be to increase the purity of the oxygen produced in the ASU. It was estimated that, by increasing the purity of the oxygen from 95% to 98.5%, requiring a slight increase in ASU consumption (Hu, 2011), the final CO_2 purity can be increased to 98.2%, with a minor effect on the complete plant efficiency.

As far as other emissions are concerned, it is very important to recall that IGCLC configurations do not produce any nitrogen oxide, because a high temperature combustion process is totally absent. This relevant benefit is not shared by the benchmark configurations (with or without CO_2 capture), where hydrogen-laden fuel combustion brings about very high flame temperatures and, potentially, abundant thermal NO_x formation, requiring strong dilution by nitrogen and/or steam to control it.

In order to assess the effects of some important design parameters, a sensitivity analysis has been performed, which is presented and discussed in the following sections. In particular, the effects of the following parameters have been evaluated:

- CLC pressure, i.e. the pressure ratio of the gas turbine cycle, which has been varied from 11 to 23 bar.
- Steam cycle pressure levels: starting from the reference values of 144 bar and 36 bar for HP and IP levels, the steam cycle HP level has been increased to 170 bar and decreased to 120 bar, while the IP has been changed to 54 bar and 20 bar.
- Increased exhaust gas recirculation for syngas dilution has been assessed by increasing the recirculated gas (stream #30 in Fig. 4) to fresh syngas (stream #27) mass flow ratio up to 3. Dilution with steam has also been considered, to achieve a steam to fresh syngas ratio of 0.5, 0.75 and 1.

5.2.1. CLC operating pressure

The pressure ratio is one of the most important parameters in the optimization of gas cycles. Here the maximum gas cycle pressure corresponds to the CLC unit pressure, which was varied to find the maximum plant efficiency. This optimization is also justified by the fact that commercial gas turbines can be hardly used "as is" in this plant and some changes to the geometry of the commercial

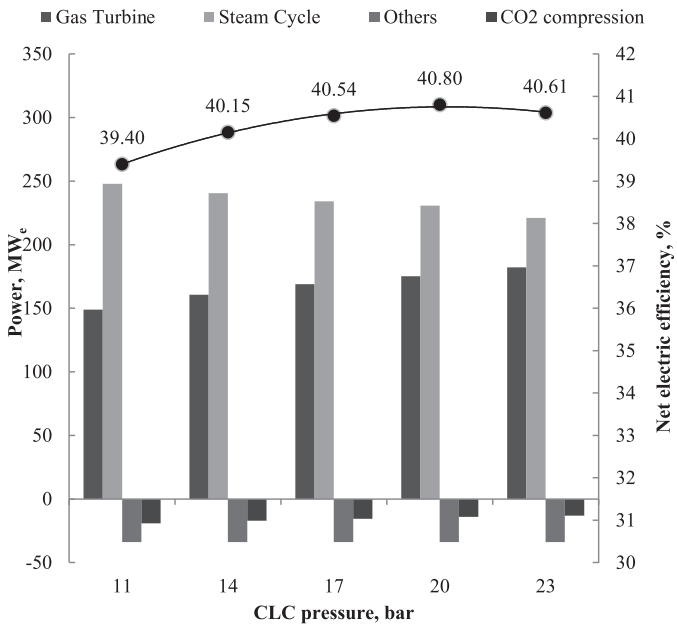

Fig. 6. Power distribution and net electric efficiencies of the IGCLC plant with co-current feeding at different pressures of the CLC unit.

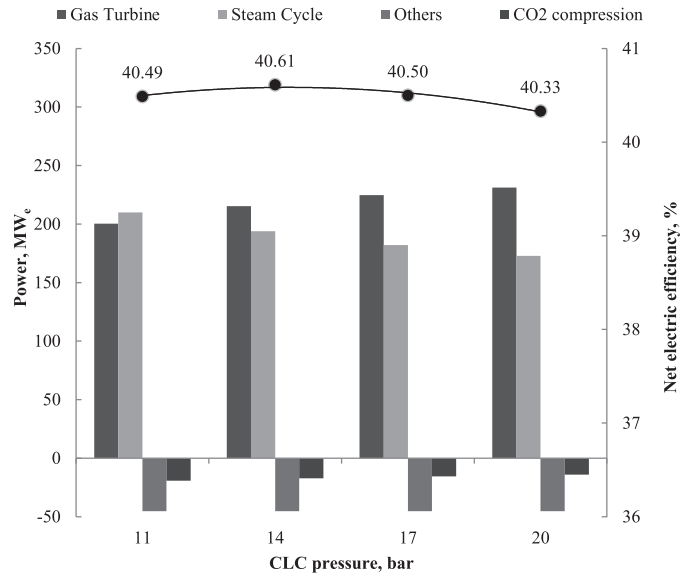

Fig. 7. Power distribution and net electric efficiencies of the IGCLC plants with counter-current feeding at different pressures of the CLC unit.

turbomachines (e.g. relative size between compressor and turbine) will be needed. Therefore, designing the adapted machine for optimal plant performance seems reasonable also from an economic point of view. Furthermore, the CLC operating pressure corresponds to the pressure of the CO_2 produced, affecting the consumptions of the downstream CO_2 compression.

The net electric efficiency and the main contributions to power production/consumption for the plant with co-current CLC feeding are shown in Fig. 6. The optimal pressure of the CLC unit maximizing the net electric efficiency is 20 bar. A maximum efficiency of 40.8% has been obtained, 0.35 percentage points higher than the base case previously discussed. By increasing the maximum pressure, the gas turbine power output increases, the bottoming steam cycle output reduces, the CO_2 compression power decreases, while the consumption of other auxiliaries remains almost constant.

The increase in the gas turbine power output over the range considered is due to both the increase in the specific work (i.e. the work per kg of air + N_2 at compressors inlet, which increases from 249 to 259 kJ/kg when the maximum pressure is increased from 11 to 23 bar) and, mainly, the increase in the N_2 flow rate. This increase is related to the higher initial temperature of N_2 and oxidation air, resulting from a higher compressor outlet pressure. The larger sensible heat introduced in the CLC system with these streams calls for higher flow rates to remove the heat released by fuel oxidation in the CLC system.

On the other hand, the steam turbine gross power production decreases (from 252 to 225 MW_e) by increasing the CLC unit pressure. The main reason is the reduced steam production in the HRSG for N_2 cooling, as a consequence of the lower turbine outlet temperature at increased expansion ratios. However, despite the lower steam generation, the overall efficiency of the steam cycle remains high, since the maximum temperature of 565 °C can be kept for the SH and RH steam. As a matter of fact, thanks to the high integration of the steam cycle, the maximum steam temperature is achieved in the CO_2/H_2O heat recovery boiler and is thus unaffected by the gas turbine outlet temperature.

Finally, the positive effect of the maximum pressure on the CO_2 compressor consumption should also be mentioned, which decreases from 19.2 to 13.0 MW_e (including also the CO_2 re-compression from the lock-hoppers recovery which accounts for 13–22% of the total consumption).

Similar trends have been obtained in the case with CLC counter-current feeding (Fig. 7). However, the penalty to the steam cycle power output at a higher pressure ratio is higher for this case because the maximum steam temperature depends on the gas turbine outlet temperature, since steam superheating and reheating are exclusively obtained by gas turbine exhaust cooling. The reduced maximum steam temperature (from 553 °C at CLC system pressure of 11 bar to 445 °C at 20 bar) is hence responsible for the decreased steam cycle efficiency with a more pronounced power output decay than in the CLC with co-current feeding.

As a result, a lower optimal CLC unit pressure than in the co-current cases has been obtained for counter-current feeding. This is equal to 14 bar, leading to a net electric efficiency of 40.61%, 0.1 percentage points higher than the base case. As a final consideration, it should be highlighted that an economic analysis is required to define the optimal economic CLC unit pressure, since reactor size and overall footprint can be affected significantly by the system pressure.

5.2.2. Sensitivity analysis on steam cycle pressure levels

Starting from the base cases with sub-optimal (but reasonably close to the optimum) CLC process pressure of 17 bar, a sensitivity analysis on the steam cycle pressure levels has been carried out. The high pressure level has been varied between 120 and 170 bar, showing a limited effect on the net plant efficiency. The effect is more pronounced for the CLC plant with co-current feeding, which is characterized by a heat source with a higher average temperature and can hence take better advantage from variations in the maximum steam cycle pressure. For this plant, increasing the maximum pressure up to 170 bar leads to an efficiency increase of 0.23 percentage points, while a decrease to 120 bar leads to a decrease of nearly 0.3 percentage points. On the contrary, a negligible effect has been obtained for the plant with counter-current feeding of the CLC unit, with variations of less than 0.1 percentage points in the pressure range considered. Variations of the intermediate pressure level between 20 and 54 bar led to lower variations of the net efficiency, with maximum differences of about 0.15 percentage points for both plant configurations.

Table 6
Thermodynamic properties of the streams reported in Fig. 4 and Fig. 5.

	T	P	m	MW	Q	Stream composition (vol. basis)									HHV	LHV
	°C	bar	kg/s	kg/kmol	kmol/s	Ar	CO	CO_2	H_2	H_2O (g)	H_2S	N_2	O_2	H_2O (l)	MJ/kg	MJ/kg
#1	25.0	1.0	516.9	28.0	18.4	1.2	–	–	–	1.3	–	97.5	–	–		
#2	466.7	20.0	467.3	28.0	16.7	1.2	–	–	–	1.3	–	97.5	–	–		
#3	510.8	20.0	573.0	28.0	20.4	1.2	–	–	–	1.3	–	97.5	–	–		
#4	1185.6	18.5	603.0	28.0	21.5	1.2	–	–	–	1.3	–	97.5	–	–		
#5	479.4	1.1	652.6	28.0	23.3	1.2	–	–	–	1.3	–	97.5	–	–		
#6	100.0	1.0	135.7	28.0	4.8	1.2	–	–	–	1.3	–	97.5	–	–		
#7	15.0	1.0	176.2	28.9	6.1	0.9	–	–	–	1.1	–	77.3	20.7	–		
#8	450.4	21.0	176.2	28.9	6.1	0.9	–	–	–	1.1	–	77.3	20.7	–		
#9	650.0	20.0	135.7	28.0	4.8	1.2	–	–	–	1.3	–	97.5	–	–		
#10	466.7	20.0	30.0	28.0	1.1	1.2	–	–	–	1.3	–	97.5	–	–		
#11	1200.0	18.5	30.0	28.0	1.1	1.2	–	–	–	1.3	–	97.5	–	–		
#12	15.0	1.0	120.7	28.9	4.2	0.9	–	–	–	1.1	–	77.3	20.7	–		
#13	15.0	48.5	28.9	32.2	0.9	3.1	–	–	–	0.0	–	1.9	95.0	–		
#14	180.0	48.0	28.9	32.2	0.9	3.1	–	–	–	0.0	–	1.9	95.0	–		
#15	80.0	56.0	23.7	43.6	0.5	1.5	–	96.6	–	0.0	–	1.9	–	–		
#16	122.3	56.0	2.4	28.0	0.1	–	–	–	–	–	–	100	–	–		
#17	30.0	1.0	13.1	43.6	0.3	1.5	–	96.6	–	0.0	–	1.9	–	–		
#18	81.6	1.0	4.7	34.1	0.1	0.6	–	37.8	–	0.0	–	61.6	–	–		
#19	30.0	88.0	2.7	43.6	0.1	1.5	–	96.6	–	0.0	–	1.9	–	–		
#20	15.0	–	34.1	–	–	*Douglas premium coal*									26.0	25.0
#21	900.0	44.0	127.4	22.6	5.6	1.0	57.4	8.4	23.4	8.4	0.2	1.2	–	–	10.4	9.7
#22	300.0	41.7	127.4	22.6	5.6	1.0	57.4	8.4	23.4	8.4	0.2	1.2	–	–	10.4	9.7
#23	210.9	44.4	60.3	22.5	2.7	0.9	53.0	8.6	21.6	14.5	0.2	1.2	–	–	9.7	9.0
#24	164.8	41.7	78.9	22.3	3.5	0.9	51.5	8.5	21.0	16.7	0.2	1.2	–	–	9.6	8.8
#25	35.0	38.8	68.2	23.2	2.9	1.1	61.8	10.2	25.2	0.1	0.2	1.4	–	–	10.7	10.2
#26	115.6	20.6	72.3	22.8	3.2	1.0	56.8	9.3	23.1	8.5	–	1.3	–	–	10.1	9.5
#27	300.0	20.4	72.3	22.8	3.2	1.0	56.8	9.3	23.1	8.5	–	1.3	–	–	10.1	9.5
#28	517.0	20.0	150.2	28.0	5.4	1.0	33.5	32.5	13.7	18.0	–	1.3	–	–	5.1	4.6
#29	1156.5	19.0	190.7	35.5	5.4	1.0	0.1	66.0	0.02	31.6	–	1.3	–	–	0.4	0.0
#30	362.3	18.8	77.9	35.5	2.2	1.0	0.1	66.0	0.02	31.6	–	1.3	–	–	0.4	0.0
#31	35.0	18.0	112.8	35.5	3.2	1.0	0.1	66.0	0.02	0.3	–	1.3	–	31.3	0.3	0.0
#32	27.8	110.0	81.3	43.6	1.9	1.4	0.2	96.4	0.03	–	–	1.8	–	–	0.3	0.0
#33	60.0	20.8	0.7	23.2	0.0	1.1	62.0	10.2	25.2	0.1	–	1.4	–	–	10.7	10.2
#34	400.0	166.6	81.6	18.0	4.5	–	–	–	–	100	–	–	–	–		
#35	454.4	164.0	41.9	19.0	2.2	–	–	–	–	100	–	–	–	–		
#36	565.0	158.1	145.2	21.0	6.9	–	–	–	–	100	–	–	–	–		
#37	337.7	36.1	145.2	22.0	6.6	–	–	–	–	100	–	–	–	–		
#38	557.4	33.1	154.2	18.0	8.6	–	–	–	–	100	–	–	–	–		
#39	32.2	0.0	151.8	18.0	8.4	–	–	–	–	100	–	–	–	–		
#40	244.2	54.0	6.7	18.0	0.4	–	–	–	–	–	–	–	–	100		
#41	300.0	52.9	2.9	18.0	0.2	–	–	–	–	100	–	–	–	–		
#42	262.9	4.0	2.3	18.0	0.1	–	–	–	–	100	–	–	–	–		

These results demonstrate that a full optimization of the pressure levels of the assessed plants should not lead to important variations of the final performance and that the assumed values are reasonably close to the optimal ones. The properties of the selected streams in Figs. 4 and 5, for the optimal co-current system case with CLC pressure of 20 bar and maximum HP steam pressure of 170 bar, are shown in Table 6.

5.2.3. *Syngas humidification*

The syngas used in the PBR is mixed with some recirculated oxidation products before being fed to the CLC reactor for the reduction phase. The syngas coming from the gasification island is rich in CO and H_2 and the recycle of CO_2 and H_2O helps preventing carbon deposition and solid over-reduction to metallic iron, which would induce agglomeration of the oxygen carrier.

The carbon deposition phenomena with syngas are mostly favored when high carbon activity is combined with local temperatures in the 400–800 °C range, at which the kinetics of the Boudouard reaction (Eq. (2)) is sufficiently fast. In the packed bed CLC system, such conditions can take place in the heat front region during the reduction phase, where no oxygen can be released by the OC completely reduced to FeO and the bed temperature steeply varies between 400/450 °C and 1200 °C. In order to understand the conditions under which these phenomena can occur, experimental analyses testing reaction kinetics and the effect of trace species like H_2S would be of primary importance to define safe operating conditions.

$$2CO \rightarrow C + CO_2 \tag{2}$$

Oxygen carrier over-reduction to metallic iron is possible under high partial pressures of the reducing species (H_2 and CO) and it can be prevented by increasing the content of H_2O and CO_2 (Campos, 2013; Leion et al., 2008). In this work a recycle rate leading to a CO content of 34% (vol. basis) has been assumed in the base cases and this sensitivity analysis explores the plant performance in case higher dilution is needed to avoid these reactions. The first option to increase the syngas dilution is to increase the recycle rate, which has been increased in order to reduce the CO content to 20 vol.% (or the CO + H_2 content to 28 vol.%, from the initial 47.4%). The simplest effect of the increased recycle rate is the increase of the recycle fan auxiliary consumption, rising from the reference 1.21 MW_e to 3.2 MW_e in the case with co-current CLC feeding. The second effect is that the increase of the gas flow rate in the reduction stage leads to increased flow of CO_2/H_2O from the CLC unit and hence higher sensible heat extracted with this stream and recovered by the bottoming steam cycle. As a consequence, the steam turbine power increases from 242 to 270 MW_e in the case with co-current

CLC feeding while the flow rate of the N_2 stream used in the heat removal step reduces from 488 to 346 kg/s. In this way, the power generated by the more efficient topping gas cycle decreases from 169 to 127 MW_e (including the air compressor). The resulting plant electric efficiency decreases from 40.5% to 38.5%.

When the same analysis is carried out for the case with counter-current CLC feeding, the increase in the recirculating gas flow rate does not significantly affect the energy balance of the system because the CO_2/H_2O stream is released from the system at relatively low temperature. As a consequence, the N_2 mass flow rate used for the heat removal only slightly decreases from 717 kg/s of the reference case to 707.5 kg/s in the case with the highest recirculation and the gas cycle power reduces from 225 to 222 MW_e. The resulting efficiency decay is hence moderate (−0.27 percentage points) and mainly associated to the increased consumption of the recycle fan.

The second option to dilute syngas is using steam extracted from the steam cycle. In this case, steam-to-syngas mole ratios of 0.5 and 1 have been tested (able to avoid C deposition at 760 °C and 670 °C respectively according to thermodynamic equilibrium). The efficiency penalty becomes more relevant because a strong reduction of the steam turbine power output is obtained. If a steam-to-syngas ratio of 0.5 is considered, the H_2O content at the reactor inlet becomes 42.8% increasing up to 58.8% in case of a steam-to-syngas ratio equal to 1. The net electric efficiency drops from to 40.5% (in the reference case) to 33.6% because the gross electric power from steam turbine decreases by as much as 45 MW_e. It has to be highlighted that the simulations at increased steam dilution have been calculated with the same plant configuration and assumptions made for the reference case. However, the efficiency penalty could be partly reduced by properly modifying the plant configuration, for example by using water at higher temperature for syngas saturation or by including a low pressure level in the steam cycle to recover the increased heat from water condensation in the CO_2/H_2O stream.

As a final comment, it should be noted that increased fuel mass flow rates to the reactor would result in a higher pressure drop or require a larger number of parallel reactors of a given size to obtain the specified pressure drop. The calculations carried out in this work do not consider these issues, which would need a definition of reactor sizing criteria, which are beyond the scope of this work.

6. Conclusions

The present work investigated two different configurations to utilize packed bed reactors for chemical looping combustion in integrated coal gasification-based combined cycle power plants. The CLC system appears as a promising option for high efficiency and high CO_2 capture power plants. The use of PBR for CLC process seems a good alternative to fluidized beds, especially for pressurized systems, even if some drawbacks and technological challenges (viz. high temperature valves and piping) need further investigation. Effects of dynamic operation can be handled by a proper heat management strategy. Different reactors operated in parallel have to be used to reduce the temperature variation of the gases produced by the system and processed by the downstream equipment.

The thermodynamic analysis of an integrated gasification CLC (IGCLC) plant has been presented discussing the plant layout and the set of assumptions used to model the CLC system and of the other main units. The proposed IGCLC system can reach an electric efficiency in the range of 40–41%, with CO_2 capture efficiencies in the order of 96%. A high CO_2 purity of 96.5% mol has been estimated with no need of any purification step. Purities higher than 98% could easily be reached, by producing oxygen at a higher purity (98.5%), which would not require a significant increase of ASU cost and consumptions.

Two configurations have been considered for the feeding of the CLC reactors: the co-current feeding system, where syngas is fed to the CLC reactors from the same side as the oxidant, and the counter-current configuration. The PBR system with co-current gas feeding configuration showed the best performance thanks to the efficient heat recovery and steam cycle integration. For the case of the counter-current configuration that requires a larger number of high temperature valves, slightly lower efficiencies were predicted, with a possibly simpler steam cycle integration.

The sensitivity analyses have shown that with the co-current configuration, the optimal operating pressure of the CLC unit is 20 bar, while for the counter-current feeding case the highest efficiency is achieved when the system is operated at 14 bar. The steam cycle evaporating pressures was found to have a very limited influence on the plant performance both for the high pressure (±0.3 percentage points in the range assessed), and the intermediate pressure levels.

The effect of different syngas dilution levels to reduce the risk of carbon deposition and metal dusting has also been assessed. In case of syngas dilution with recirculated exhaust gases, the efficiency drop can be up to 2 percentage points for the co-current configuration as the CO_2 content in the fuel stream is taken down to 20 vol.%. For the counter-current configuration a moderate effect has been calculated (less than 0.3 percentage points). In case of syngas dilution with steam extracted from the steam cycle, the efficiency drops are relevant, leading to a significant loss of competitiveness with respect to other technologies. Therefore, experimental studies aimed at assessing the risk and the effects on the oxygen carrier of carbon deposition would be extremely important for a correct evaluation of the performance of the IGCLC concept.

In comparison with conventional pre-combustion capture from IGCC with solvents, the systems here proposed show a consistently lower SPECCA index (1.1 vs. 3.3 MJ_{LHV}/kg_{CO_2}). This difference may however reduce somewhat (1.7 vs. 3.1 MJ_{LHV}/kg_{CO_2}), if advanced gas turbines are developed by manufacturers, i.e. the same TIT of conventional natural gas-fired machines can be reached with H_2 and syngas as fuels. In this case, the efficiencies of the benchmark cases would improve, while IGCLC plants would not get any benefits, since the maximum cycle temperature is limited by the oxygen carrier resistance.

As far as economics are concerned, the expected performance of the IGCLC plants will affect the operating cost. However, to figure out the real impact of IGCLC commercialization, an economic assessment and comparisons with other technologies are required. In the specific case of IGCLC, the cost of the reactor network (vessels, valves and piping) should not overstep a certain value to be competitive with pre-combustion capture technologies. A more detailed work discussing the reactor design and the associated cost for a large scale implementation will be presented in a future work.

Acknowledgement

The research leading to these results has received funding from the European Union Seventh Framework Programme (FP7/2007–2013) under grant agreement n° 268112 (Project acronym DEMOCLOCK).

References

Abad, A., Adánez-Rubio, I., Gayán, P., García-Labiano, F., de Diego, L.F., Adánez, J., 2012. Demonstration of chemical-looping with oxygen uncoupling (CLOU) process in a 1.5 kWth continuously operating unit using a Cu-based oxygen-carrier. Int. J. Greenh. Gas Control 6, 189–200.

Adanez, J., Abad, A., Garcia-Labiano, F., Gayan, P., de Diego, L., 2012. Progress in chemical-looping combustion and reforming technologies. Prog. Energy Combust. Sci. 38, 215–282.

Andrus, H., Chiu, J., Thibeault, P., Brautsch, A., 2009. Alstom's calcium oxide chemical looping combustion coal power technology development. In: 34th International Technical Conference on Clean Coal & Fuel System, Florida, USA.

Brandvoll, O., Bolland, O., 2004. Inherent CO_2 capture using chemical looping combustion in a natural gas fired power cycle. J. Eng. Gas Turbines Power 126, 316.

Campos, D.C., 2013. Reactivity investigation on iron-titanium oxides for a moving bed chemical looping combustion implementation. Adv. Chem. Eng. Sci. 03, 47–56.

Chiesa, P., Lozza, G., Malandrino, A., Romano, M., Piccolo, V., 2008. Three-reactors chemical looping process for hydrogen production. Int. J. Hydrogen Energy 33, 2233–2245.

Chiesa, P., Macchi, E., 2004. A thermodynamic analysis of different options to break 60% electric efficiency in combined cycle power plants. J. Eng. Gas Turbines Power 126, 770.

Consonni, S., Lozza, G., Pelliccia, G., Rossini, S., Saviano, F., 2006. Chemical-looping combustion for combined cycles with CO_2 capture. J. Eng. Gas Turbines Power 128, 525.

EBTF, 2011. European Best Practice Guidelines for Assessment of CO_2 Capture Technologies. http://www.gecos.polimi.it/research/EBTF_best_practice_guide.pdf

Erlach, B., Schmidt, M., Tsatsaronis, G., 2011. Comparison of carbon capture IGCC with pre-combustion decarbonisation and with chemical-looping combustion. Energy 36, 3804–3815.

Democlock, EU FP7 project, grant agreement n. 268112, 2011–2015. http://www.sintef.no/Projectweb/DemoClock/

Gallucci, F., van Sint Annaland, M., 2011. A review on recent patents on chemical and calcium looping processes. Recent Pat. Chem. Eng. 4, 280–290.

Gecos, 2013. Gas–Steam Cycle Simulation Code. http://www.gecos.polimi.it/software/gs.php

Hamers, H.P., Gallucci, F., Cobden, P.D., Kimball, E., van Sint Annaland, M., 2013. A novel reactor configuration for packed bed chemical-looping combustion of syngas. Int. J. Greenh. Gas Control 16, 1–12.

Hu, Y., 2011. CO_2 capture from oxy-fuel combustion power plants. KTH Royal Institute of Technology.

IEA, 2008. World Energy Outlook.

IEAGHG, 2005. Oxy Combustion Processes for CO_2 Capture from Power Plant.

IEA, UNIDO, 2011. Technology Roadmap Carbon Capture and Storage in Industrial Applications.

Ishida, M., Zheng, D., Akehata, T., 1987. Evaluation of a chemical-looping-combustion power-generation system by graphic exergy analysis. Energy 12, 147–154.

Ishida, M., Jin, H., 1994. A new advanced power-generation system using chemical-looping combustion. Energy 19, 415–422.

Jerndal, E., Mattisson, T., Lyngfelt, A., 2006. Thermal analysis of chemical-looping combustion. Chem. Eng. Res. Des. 84, 795–806.

Kolbitsch, P., Bolhàr-Nordenkampf, J., Pröll, T., Hofbauer, H., 2010. Operating experience with chemical looping combustion in a 120 kW dual circulating fluidized bed (DCFB) unit. Int. J. Greenh. Gas Control 4, 180–185.

Leion, H., Lyngfelt, A., Johansson, M., Jerndal, E., Mattisson, T., 2008. The use of ilmenite as an oxygen carrier in chemical-looping combustion. Chem. Eng. Res. Des. 86, 1017–1026.

Lewis, W.K., Gilliland, E.R., 1954. Production of Pure Carbon Dioxide. 2,665,971.

Linderholm, C., Lyngfelt, A., Cuadrat, A., Jerndal, E., 2012. Chemical-looping combustion of solid fuels – operation in a 10 kW unit with two fuels, above-bed and in-bed fuel feed and two oxygen carriers, manganese ore and ilmenite. Fuel 102, 808–822.

Lozza, G., Chiesa, P., Romano, M.C., Savoldelli, P., 2006. Three reactors chemical looping combustion for high efficiency electricity generation with CO_2 capture from natural gas. In: Proc. ASME Turbo Expo, pp. 1–11, GT2006-90345.

Metz, B., Davidson, O., Coninck, H., de Loos, M., Meyer, L., 2005. IPCC Special Report on Carbon Dioxide Capture and Storage.

Naqvi, R., Bolland, O., 2007. Multi-stage chemical looping combustion (CLC) for combined cycles with CO_2 capture. Int. J. Greenh. Gas Control 1, 19–30.

Naqvi, R., Wolf, J., Bolland, O., 2007. Part-load analysis of a chemical looping combustion (CLC) combined cycle with CO_2 capture. Energy 32, 360–370.

Noorman, S., Gallucci, F., van Sint Annaland, M.J., Kuipers, A.M., 2011. A theoretical investigation of CLC in packed beds. Part 2: Reactor model. Chem. Eng. J. 167, 369–376.

Rezvani, S., Huang, Y., McIlveen-Wright, D., Hewitt, N., Mondol, J.D., 2009. Comparative assessment of coal fired IGCC systems with CO_2 capture using physical absorption, membrane reactors and chemical looping. Fuel 88, 2463–2472.

Sit, S., Reed, A., Hohenwarter, U., Horn, V., Marx, K., Pröll, T., 2012. 10 MW CLC field pilot. In: Proceedings of the 2nd International Conference on Chemical Looping, Darmstadt, Germany, 26–28 September.

Son, S., Kim, S., 2006. Chemical-looping combustion with NiO and Fe_2O_3 in a thermobalance and circulating fluidized bed reactor with double loops. Ind. Eng. Chem. Res. 45, 2689–2696.

Sorgenfrei, M., Tsatsaronis, G., 2014. Design and evaluation of an IGCC power plant using iron-based syngas chemical-looping (SCL) combustion. Appl. Energy 113, 1958–1964.

Spallina, V., Gallucci, F., Romano, M.C., Chiesa, P., Lozza, G., van Sint Annaland, M., 2013a. Investigation of heat management for CLC of syngas in packed bed reactors. Chem. Eng. J. 225, 174–191.

Spallina, V., Romano, M.C., Chiesa, P., Lozza, G., 2013b. Integration of coal gasification and packed bed CLC process for high efficiency and near-zero emission power generation. Energy Proc. 37, 662–670.

Wolf, J., Anheden, M., Yan, J., 2005. Comparison of nickel- and iron-based oxygen carriers in chemical looping combustion for CO capture in power generation. Fuel 84, 993–1006.